

Surface Functionalization of Fluoroalkyl End-Capped Oligomer/Silica Nancomposites via Graft Polymerization: Application to the Dispersion of Fullerene and Single-Walled Carbon Nanotubes in Water with These Nanocomposites

Hideo Sawada,* Yuki Goto, and Tamikazu Narumi

Department of Frontier Materials Chemistry, Graduate School of Science and Technology, Hirosaki University, Hirosaki 036-8561

Received August 10, 2009; E-mail: hideosaw@cc.hirosaki-u.ac.jp

Fluoroalkyl end-capped acrylic acid oligomer/silica nanocomposites [R_F–$(ACA)_n$–R_F/SiO_2] containing vinyl (Vinyl*Si*) or methacryloyloxypropyl (MAcryl*Si*) groups were prepared by the sol–gel reactions of the corresponding fluorinated oligomer with tetraethoxysilane and silica nanoparticles in the presence of trimethoxyvinylsilane or 3-methacryloyloxypropyltrimethoxysilane under alkaline conditions, respectively. These fluorinated nanocomposites were applied to surface initiated radical copolymerization, and polystyrene (PSt) and poly(*N*,*N*-dimethylacrylamide) (PDMAA) grafted R_F–$(ACA)_n$–R_F/SiO_2 nanocomposites were prepared by the surface copolymerizations of R_F–$(ACA)_n$–R_F/SiO_2 containing Vinyl*Si* (or MAcryl*Si*) groups with styrene or *N*,*N*-dimethylacrylamide. In these nanocomposites, PSt–Vinyl*Si* grafted R_F–$(ACA)_n$–R_F/SiO_2 nanocomposite, which was prepared by the surface copolymerization of R_F–$(ACA)_n$–R_F/SiO_2 containing Vinyl*Si* groups with styrene, are useful for a new fluorinated polysoap, and this nanocomposite was the most effective for the dispersion of fullerene and single-walled carbon nanotubes into water.

Surface modification of silica nanoparticles by chemically bound polymers is of great interest due to their potential applications in a wide variety of fields such as coatings, electronics, catalysis, optics, and diagnostics.[1] There have been numerous reports on the preparation of polymer grafted silica nanoparticles by the use of free radical polymerization,[2] cationic and anionic polymerization,[3] miniemulsion polymerization,[4] living radical polymerizations such as RAFT (reversible addition–fragmentation chain transfer) polymerization with click reactions,[5] nitroxide-mediated polymerization,[6] and atom-transfer radical polymerization.[7] Inorganic nanoparticles are usually utilized as the cores of grafted polymers to combine the superior properties of the organic and inorganic materials.[8] So far, fluorinated polymers have proven to be useful functional materials because of their excellent chemical and thermal stability, low surface energy, and low refractive index which cannot be achieved in the corresponding non-fluorinated polymers.[9] Therefore, it is of particular interest to explore novel fluorinated polymer grafted silica nanoparticles from the developmental viewpoints of new functional materials imparted by both fluorine and silica nanoparticles. However, these studies have been hitherto very limited, although Ober et al. reported the preparation of planar silicon oxide surface-grafted styrene-based diblock copolymer brushes bearing semifluorinated alkyl side groups by nitroxide-mediated controlled radical polymerization.[10] In our comprehensive studies on the synthesis and properties of new fluorinated polymers,[11] we have already reported that fluoroalkyl end-capped oligomers are attractive functional materials, because they exhibit various unique properties such as high solubility, surface active properties, biological activities, and nanometer size-controlled self-assembled molecular aggregates which cannot be achieved by the corresponding non-fluorinated and randomly fluoroalkylated polymers.[12] From this point of view, it is more essential to develop fluoroalkyl end-capped oligomer grafted silica nanoparticles, and we previously succeeded in preparing a variety of new fluoroalkyl end-capped oligomer grafted silica nanoparticles.[13] In these fluorinated oligomer grafted silica nanoparticles (fluorinated oligomer/silica nanocomposites), we have recently discovered that fluoroalkyl end-capped *N*-(1,1-dimethyl-3-oxobutyl)acrylamide oligomer/silica nanocomposites exhibit no weight loss corresponding to the content of fluorinated oligomer in the silica composites even after calcination at 800 °C.[14] Here we report that fluoroalkyl end-capped oligomer/silica nanoparticles can be applicable to the surface functionalization of fluorinated oligomer/silica nanocomposites by the use of surface-initiated radical polymerization. We believe that this is the first report for the surface functionalization of fluoroalkyl end-capped polymer grafted silica nanoparticles. These surface functionalized fluorinated oligomer grafted silica nanoparticles were also applied to the dispersion of fullerene and single-walled carbon nanotubes into water. These findings will be described herein.

Results and Discussion

Fluoroalkyl end-capped acrylic acid oligomer/silica nanocomposites containing vinyl groups were prepared by the sol–gel reaction of the corresponding oligomer with tetraethoxysilane and silica nanoparticles in the presence of trimethoxy-

Published on the web December 23, 2009; doi:10.1246/bcsj.20090208

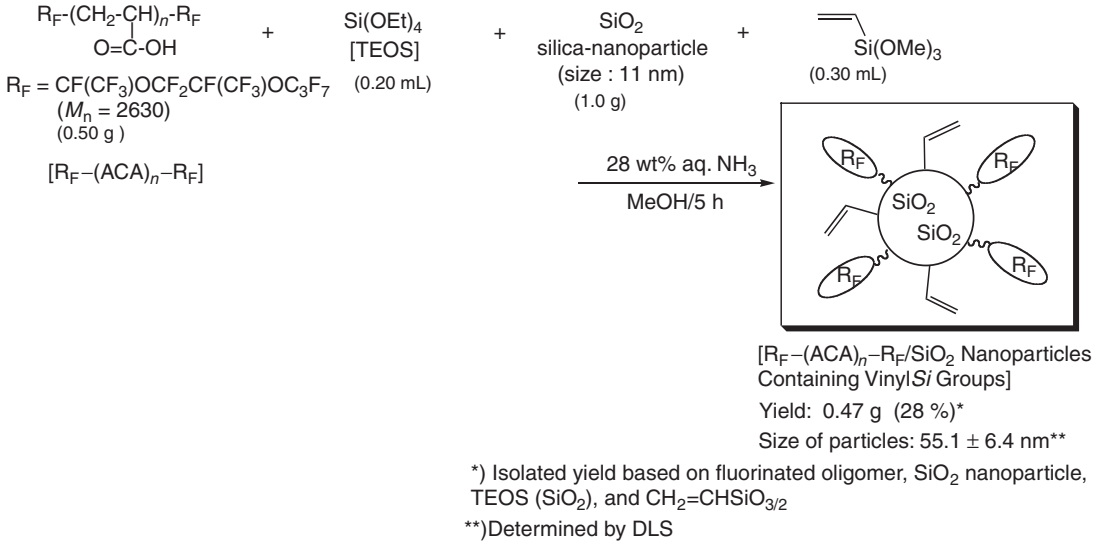

Scheme 1. Preparation of fluoroalkyl end-capped acrylic acid oligomer/SiO_2 nanoparticles containing Vinyl*Si* groups.

vinylsilane under alkaline conditions. This reaction is illustrated in Scheme 1.

As shown in Scheme 1, the sol–gel reaction proceeded smoothly under alkaline conditions to afford the expected fluoroalkyl end-capped acrylic acid oligomer/silica nanocomposites containing vinyl (Vinyl*Si*) groups in 28% isolated yield.

The fluorinated nanocomposites thus obtained were found to exhibit a good dispersibility in traditional organic solvents such as methanol, ethanol, tetrahydrofuran, and 1,2-dichloroethane including water. Thus, we have measured the size (number-average diameter) of these nanocomposites in methanol by the use of dynamic light scattering (DLS) measurements at 25 °C, and these results are also shown in Scheme 1. DLS measurements show that the composite particles are nanometer size-controlled fine particles (55.1 ± 6.4 nm). This composite exhibited a good redispersibility in methanol, and the size (47.6 ± 4.2 nm) of the redispersed composite particles did not change even after the redispersion of the parent fluorinated composite particle powders in methanol, and the particles were monodisperse.

Our present fluorinated oligomer/silica nanocomposites possess Vinyl*Si* groups on their surface. It is suggested that surface-grafted polymers such as polystyrene (PSt) and poly(*N*,*N*-dimethylacrylamide) (PDMAA) can be prepared by radical copolymerization on these fluorinated nanocomposite surfaces. In fact, we tried to prepare PSt or PDMAA grafted fluoroalkyl end-capped acrylic acid oligomer/silica nanocomposite by the radical copolymerization of the corresponding fluorinated nanocomposites containing Vinyl*Si* groups with St or DMAA comonomer initiated by azo-initiator [V-65: 2,2′-azobis(2,4-dimethylvaleronitrile)], and the results are shown in Scheme 2.

As shown in Scheme 2, surface-grafted copolymerization of fluorinated silica nanocomposites proceeded smoothly to afford PSt–Vinyl*Si* grafted fluorinated silica nanocomposites under mild conditions. This copolymerization was found to proceed more effectively by the use of fluorinated oligomeric surfactants such as fluoroalkyl end-capped *N*,*N*-dimethylacrylamide homooligomer [R_F–($CH_2CHCONMe_2$)$_n$–R_F; R_F = $CF(CF_3)OC_3F_7$; $M_n = 4820$]. In addition, the size of the obtained PSt–Vinyl*Si* grafted fluorinated silica nanocomposite was found to increase effectively from 56 to 91 nm by the use of fluorinated oligomeric surfactant. In order to clarify the contents of PSt in the composites, we have tested these nanocomposites for thermal stability by thermogravimetric analyses (TGA), in which the weight loss of these nanocomposites was measured by raising the temperatures around 800 °C at a 10 °C min^{-1} heating rate under air. These results were shown in Figure 1.

The weight of parent fluoroalkyl end-capped acrylic acid oligomer [R_F–(ACA)$_n$–R_F] markedly dropped around 255 °C and decomposed completely around 500 °C. A similar tendency was observed in R_F–(ACA)$_n$–R_F/silica nanocomposite, R_F–(ACA)$_n$–R_F/silica nanocomposite containing Vinyl*Si* groups and PSt–Vinyl*Si* grafted R_F–(ACA)$_n$–R_F/silica nanocomposites, and a constant value for their weight loss was observed above 500 °C, indicating that these nanocomposites could possess silica gel nanoparticles. In these nanocomposites, PSt–Vinyl*Si* grafted R_F–(ACA)$_n$–R_F/silica nanocomposites (B in Figure 1), which were prepared by the use of R_F–(DMAA)$_n$–R_F oligomer as the surfactant, were found to exhibit higher weight loss corresponding to the content of grafted PSt segments (10%), compared to that of R_F–(ACA)$_n$–R_F/silica nanocomposite containing Vinyl*Si* groups. In contrast, PSt–Vinyl*Si* grafted R_F–(ACA)$_n$–R_F/silica nanocomposites (A in Figure 1), which were prepared without the use of surfactant, afforded similar weight loss as that of the parent R_F–(ACA)$_n$–R_F/silica nanocomposite containing Vinyl*Si* groups (C in Figure 1), indicating that the fluorinated oligomeric surfactant is essential for the smooth graft copolymerization of styrene on the composite surface. From these weight loss results at 800 °C, we can easily estimate the contents of R_F–(ACA)$_n$–R_F oligomer (D in Figure 1), Vinyl*Si* groups (C in Figure 1), and grafted PSt segments (A and B in Figure 1) in the nanocomposites, and the contents are shown in Table 1.

We also succeeded in preparing PDMAA–Vinyl*Si* grafted R_F–(ACA)$_n$–R_F/silica nanocomposites under similar conditions as that of PSt–Vinyl*Si* grafted R_F–(ACA)$_n$–R_F/silica nanocomposites (Scheme 2).

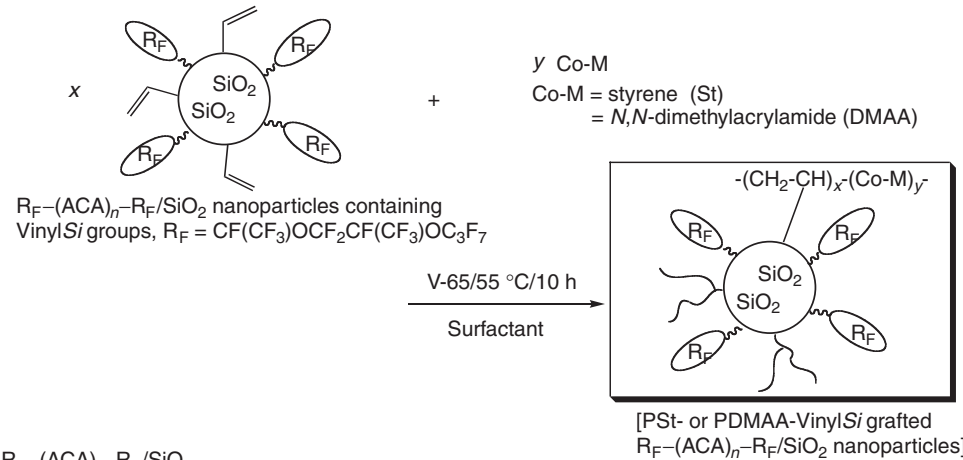

	R_F–(ACA)$_n$–R_F/SiO_2 nanoparticles containing Vinyl*Si* groups/g	Co-M (g)	V-65 /g	Surfactant /g	Yield	Size of the obtained particles**
Run 1	0.20	St (2.0)	0.3	0	0.11 g (55 %)*	55.6 ± 5.5 nm
Run 2	0.16	St (2.0)	0.3	0.4	0.14 g (88 %)*	91.0 ± 23.6 nm
Run 3	0.23	DMAA (2.0)	0.3	0	0.02 g (9 %)*	225 ± 38 nm
Run 4	0.30	DMAA (2.0)	0.3	0.4	0.13 g (43 %)*	290 ± 36 nm

*)Isolated yield base on the used R_F–(ACA)$_n$–R_F/SiO_2 nanoparticles containing Vinyl*Si* groups
**) Determined by DLS

Scheme 2. Preparation of PSt–Vinyl*Si* (or PDMAA–Vinyl*Si*) grafted fluoroalkyl end-capped acrylic acid oligomer/SiO_2 nanoparticles.

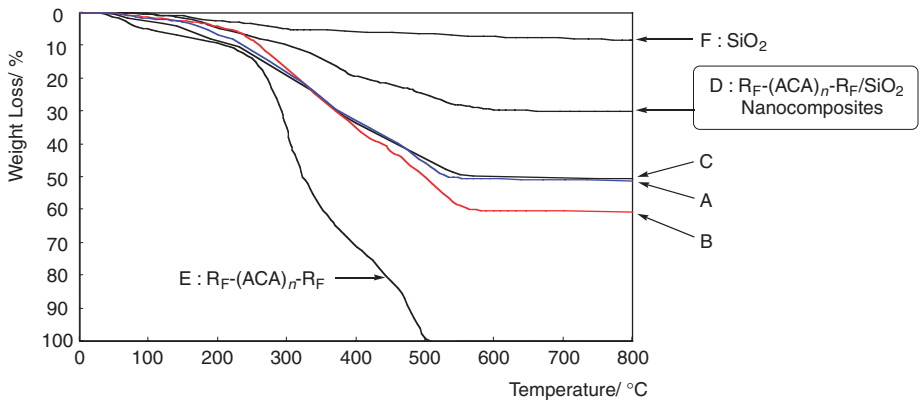

Figure 1. Thermogravimetric analyses of PSt–Vinyl*Si* grafted R_F–(ACA)$_n$–R_F/SiO_2 nanocomposites, R_F–(ACA)$_n$–R_F/SiO_2 nanocomposites containing Vinyl*Si* groups, R_F–(ACA)$_n$–R_F/SiO_2 nanocomposites, R_F–(ACA)$_n$–R_F, and SiO_2. A: PSt–Vinyl*Si* grafted R_F–(ACA)$_n$–R_F/SiO_2 nanocomposites (Run 1 in Scheme 2) B: PSt–Vinyl*Si* grafted R_F–(ACA)$_n$–R_F/SiO_2 nanocomposites [surfactant was used.] (Run 2 in Scheme 2) C: R_F–(ACA)$_n$–R_F/SiO_2 nanocomposites containing Vinyl*Si* groups.

Table 1. The Contents of R_F–(ACA)$_n$–R_F Oligomer, Vinyl*Si* Groups, and Grafted PSt Segments in the Nanocomposites

	Content/%
R_F–(ACA)$_n$–R_F oligomer	22
Vinyl*Si* segments	20
Grafted PSt segments (no surfactant)	0.8
Grafted PSt segments (surfactant)	10

However, unexpectedly surface-grafted copolymerizations of fluorinated silica nanocomposites containing Vinyl*Si* groups with DMAA monomer were not affected by the fluorinated polymeric surfactant [R_F–(DMAA)$_n$–R_F], and the size of the obtained nanocomposites and the contents of grafted PDMAA segments were almost the same in each case (each content of grafted PDMAA: 25%; see A, B in Figure 2). This suggests that DMAA monomer should interact smoothly with fluorinated silica nanocomposite surface through the intermolecular hydrogen-bonding interactions between the residual silanol groups on the silica composite surface and an amide group in DMAA monomer to give the expected PDMAA–Vinyl*Si* grafted fluorinated silica nanocomposites even without the use of fluorinated surfactants, because DMAA monomer possesses an amide group, unlike St monomer.

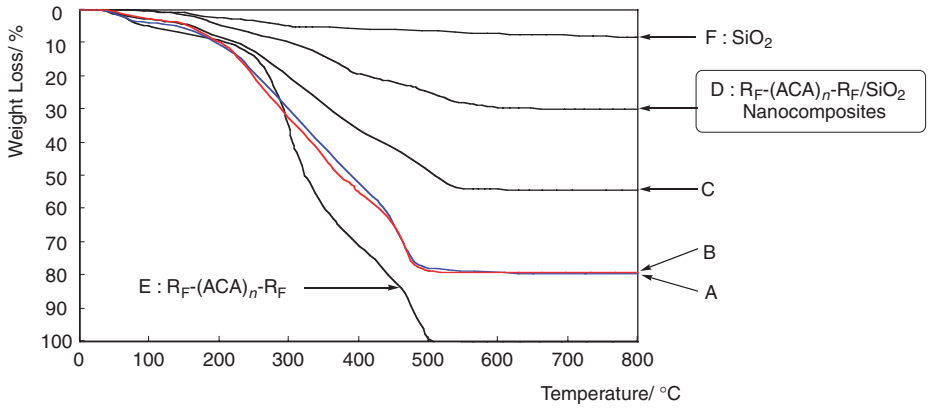

Figure 2. Thermogravimetric analyses of PDMAA–Vinyl*Si* grafted R_F–$(ACA)_n$–R_F/SiO_2 nanocomposites, R_F–$(ACA)_n$–R_F/SiO_2 nanocomposites containing Vinyl*Si* groups, R_F–$(ACA)_n$–R_F/SiO_2 nanocomposites, R_F–$(ACA)_n$–R_F, and SiO_2 A: PDMAA–Vinyl*Si* grafted R_F–$(ACA)_n$–R_F/SiO_2 nanocomposites (Run 3 in Scheme 2) B: PDMAA–Vinyl*Si* grafted R_F–$(ACA)_n$–R_F/SiO_2 nanocomposites [surfactant was used.] (Run 4 in Scheme 2) C: R_F–$(ACA)_n$–R_F/SiO_2 nanocomposites containing Vinyl*Si* groups.

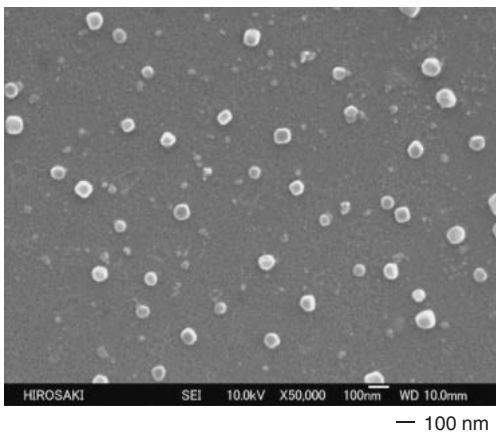

Figure 3. SEM (scanning electron microscopy) images of methanol solution of R_F–$(ACA)_n$–R_F/SiO_2 containing vinylsilyl groups.

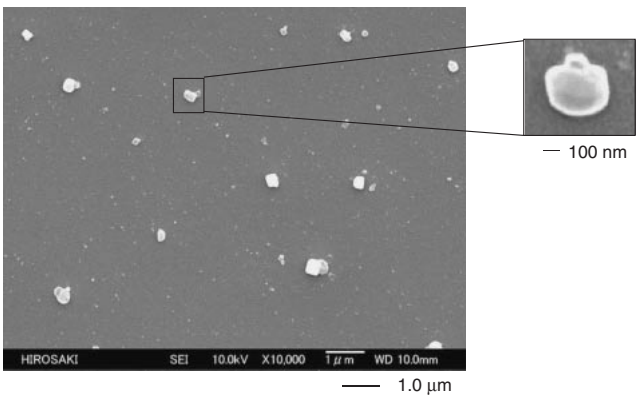

Figure 4. SEM images of methanol solution of PDMAA–Vinyl*Si* grafted R_F–$(ACA)_n$–R_F/SiO_2 nanocomposites (Run 4 in Scheme 2).

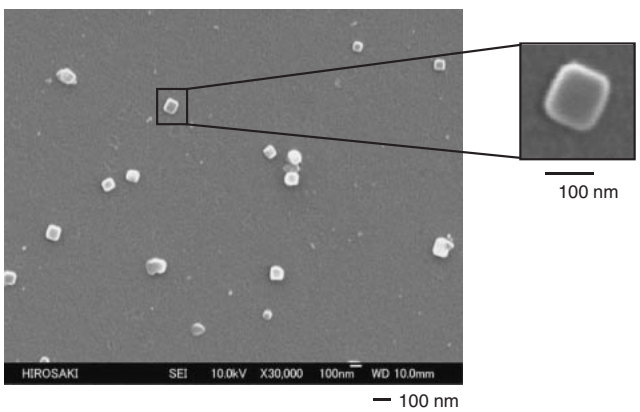

Figure 5. SEM images of methanol solution of PSt–Vinyl*Si* R_F–$(ACA)_n$–R_F/SiO_2 nanocomposites (Run 2 in Scheme 2).

The scanning electron micrograph (SEM) of R_F–$(ACA)_n$–R_F/SiO_2 nanocomposites containing Vinyl*Si* groups and PDMAA–Vinyl*Si* grafted R_F–$(ACA)_n$–R_F/SiO_2 nanocomposites (Run 4 in Scheme 2) also shows the formation of composite fine particles with a mean diameter of 71 and 238 nm, respectively (Figures 3 and 4). In addition, the average particle sizes determined by DLS (Schemes 1 and 2) were almost the same as those in the SEM images. As shown in Figure 5, we have obtained similar SEM images (mean diameter of particles: 89 nm) of PSt–Vinyl*Si* grafted R_F–$(ACA)_n$–R_F/SiO_2 nanocomposites (Run 2 in Scheme 2) to those of PDMAA–Vinyl*Si* grafted R_F–$(ACA)_n$–R_F/SiO_2 nanocomposites in Figure 4, and the cubic shape of each particle is quite different from that (spherical shape) of parent silica nanoparticles (Figure 6) and R_F–$(ACA)_n$–R_F/SiO_2 nanocomposites containing vinylsilyl groups (Figure 3). This finding also suggests that the graft reactions illustrated in Scheme 2 should proceed smoothly to afford the expected PDMAA or PSt grafted fluorinated nanocomposites.

Methacryloyloxypropyltrimethoxysilane is widely used as a radical polymerizable monomer in the formation of sol–gel composites.[15] Thus, we tried to prepare PSt or PDMAA grafted R_F–$(ACA)_n$–R_F/SiO_2 nanocomposites by the use of methacryloyloxypropyltrimethoxysilane according to the preparative conditions shown in Scheme 1. The result is shown in Scheme 3.

As shown in Scheme 3, we succeeded in preparing R_F–$(ACA)_n$–R_F/SiO_2 nanocomposites containing methacryloyl-

oxypropyl (MAcrylSi) groups. The obtained composites were found to exhibit good dispersibility and redispersibility in water, methanol, ethanol, tetrahydrofuran, and 1,2-dichloroethane. DLS measurements show that this composite is nanometer size-controlled fine particles (56.2 ± 5.7 nm) and the composite particles were monodisperse.

R_F–$(ACA)_n$–R_F/SiO_2 nanocomposite containing MAcrylSi groups was found to copolymerize with St or DMAA as comonomer in the presence of azo-initiator to afford the expected PSt or PDMAA grated R_F–$(ACA)_n$–R_F/SiO_2 nanocomposites under mild conditions (Scheme 3). These fluorinated nanocomposites thus obtained exhibited a similar dispersibility in a variety of solvents to that of parent fluorinated composite containing MAcrylSi groups. The size of these nanocomposites was found to increase effectively from 56 to 189–484 nm by graft co-polymerization, indicating that graft copolymerization should proceed smoothly on the silica composite surface as illustrated in Scheme 4.

The contents of MAcrylSi segments, grafted PSt segments and grafted PDMAA segments in the nanocomposites were estimated by the use of TGA measurements (data not shown).

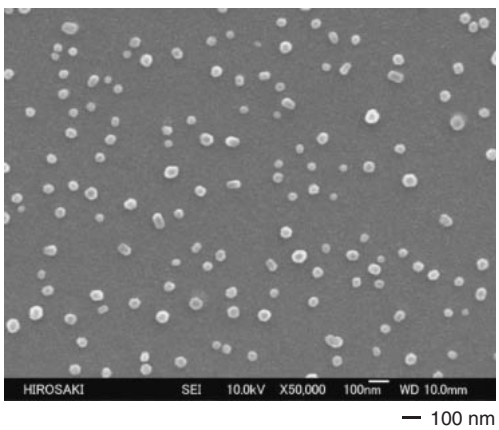

Figure 6. SEM images of methanol solution of parent SiO_2 nanocomposites.

The effective weight loss at 800 °C of these nanocomposites shows that the contents of these segments are shown in Table 2.

Interestingly, surface copolymerization of R_F–$(ACA)_n$–R_F/SiO_2 nanocomposites containing MAcrylSi groups with St or DMAA monomer was not affected at all by the fluorinated oligomeric surfactant. This finding would be due to the higher content (41%) of radical copolymerizable methacryloyloxypropyl segments in the nanocomposites, compared to that (20%) of relatively poor radical copolymerizable vinyl segments in the nanocomposites as in Scheme 1. In addition, the higher contents of grafted PDMAA segments compared to those of grafted PSt segments in the nanocomposites would be due to the effective intermolecular hydrogen-bonding interaction between the residual silanol segments on the silica nanocomposites and the amide segments in DMAA monomer during the graft copolymerization. We have observed the gel formation of PDMAA–MAcrylSi grafted R_F–$(ACA)_n$–R_F/SiO_2 nanocomposites in methanol, although the corresponding PDMAA–VinylSi grafted fluorinated nanocomposites cannot cause the gel formation to afford a well-dispersed methanol solution. This would be due to the higher grafting ratios on the PDMAA–MAcrylSi grafted R_F–$(ACA)_n$–R_F/SiO_2 nanocomposites.

We have measured the mean ζ-potential of well-dispersed aqueous solutions containing PSt and PDMAA grafted fluorinated nanocomposites in order to clarify the surface morphology of these nanocomposites, and the results are shown in Table 3.

The mean ζ-potential of original fluorinated nanocomposite containing VinylSi and MAcrylSi groups was negatively enhanced charge: -54.2–-55.7 mV compared to that (-3.67 mV) of the parent silica nanoparticles (particle size: 11 nm), indicating that negatively charged carboxyl groups in the composites should be arranged on the composite particle surface. The effective decrease of the negatively charged values from -54.2 to -33.0–-46.7 mV or from -55.7 to -36.1–-37.2 mV after graft reactions demonstrates that the graft copolymerization of St or DMAA monomer can surely proceed on the particle surfaces.

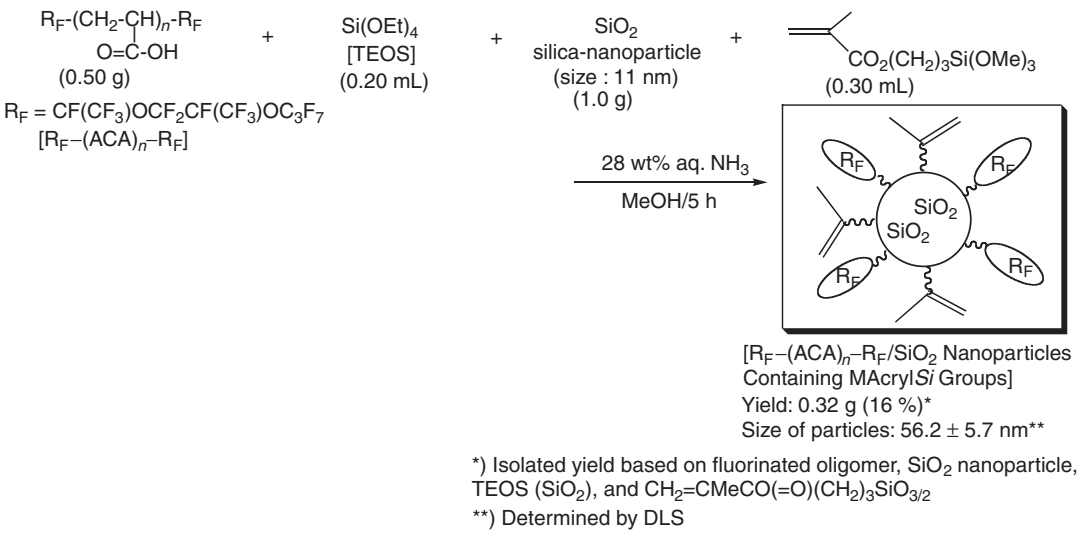

Scheme 3. Preparation of fluoroalkyl end-capped acrylic acid oligomer/SiO_2 nanoparticles containing MAcrylSi groups.

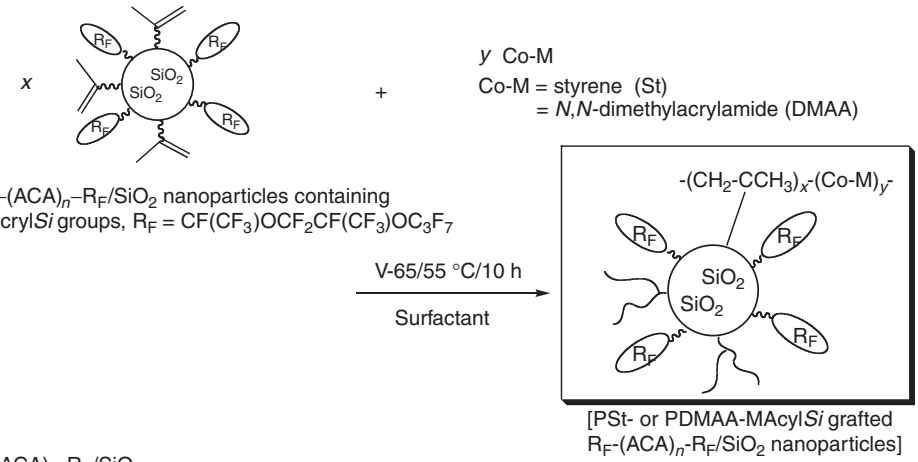

	R_F-$(ACA)_n$-R_F/SiO_2 nanoparticles containing MAcrylSi groups/g	Co-M (g)	V-65 /g	Surfactant /g	Yield	Size of the obtained particles**
Run 1	0.22	St (2.0)	0.3	0	0.07g (32 %)*	277 ± 46 nm
Run 2	0.19	St (2.0)	0.3	0.4	0.18 g (95 %)*	484 ± 117 nm
Run 3	0.32	DMAA (2.0)	0.3	0	0.14 g (44 %)*	189 ± 55 nm
Run 4	0.32	DMAA (2.0)	0.3	0.4	0.14 g (44 %)*	203 ± 45 nm

*)Isolated yield base on the used R_F–$(ACA)_n$–R_F/SiO_2 nanoparticles containing MAcrylSi groups
**) Determined by DLS

Scheme 4. Preparation of PSt–MAcrylSi (or PDMAA–MAcrylSi) grafted fluoroalkyl end-capped acrylic acid oligomer/SiO_2 nanoparticles.

Table 2. The Contents of MAcrylSi Segments, Grafted PSt Segments, and Grafted PDMAA Segments in the Nanocomposites

	Content/%
MAcrylSi segments	41
Grafted PSt segments (no surfactant)	7
Grafted PSt segments (surfactant)	6
Grafted PDMAA segments (no surfactant)	26
Grafted PDMAA segments (surfactant)	28

Table 3. Particle Size of PSt and PDMAA Grafted Fluorinated Nanocomposites and the Mean ζ-Potential of Well-Dispersed Aqueous Solutions Containing the Nanocomposites

Composites	Particle size /nm	The ζ-potential /mV
Original SiO_2 nanoparticles	11	−3.67
PSt–VinylSi grafted composite	91	−33.0
PDMAA–VinylSi grafted composite	290	−46.7
PSt–MAcrylSi grafted composite	484	−36.1
PDMAA–MAcrylSi grafted composite	203	−37.2
Original composite containing VinylSi groups	55	−54.2
Original composite containing MAcrylSi groups	37	−55.7

Our present PSt or PDMAA grafted R_F–$(ACA)_n$–R_F/SiO_2 nanocomposites are expected to be applicable to a new fluorinated polysoap. These fluorinated nanocomposites should open new development in the dispersion of guest molecules such as fullerene and carbon nanotubes, which in general exhibit extremely poor dispersibility in water, through the encapsulation of guest molecules into the fluorinated copolymeric networks in aqueous media. Hitherto, it has been reported that nanometer size-controlled self-assembled molecular aggregates formed by two fluoroalkyl end-capped oligomers such as R_F–$(CH_2CHCOOH)_n$–R_F (R_F = fluoroalkyl groups) could provide suitable host moieties to interact with guest molecules such as fullerene and single-walled carbon nanotubes (SW-CNT) in aqueous solutions.[16] Therefore, it is of particular interest to study the dispersion of fullerene and SW-CNT into water by the use of PSt and PDMAA grafted R_F–$(ACA)_n$–R_F/SiO_2 nanocomposites. In fact, we have studied the dispersion of fullerene and SW-CNT into water by using these nanocomposites, and the dispersion with R_F–$(ACA)_n$–R_F/SiO_2 nanocomposites containing VinylSi groups or MAcrylSi groups was also studied under similar conditions, for comparison. These results are shown in Figures 7–9.

Well-dispersed PSt–VinylSi grafted R_F–$(ACA)_n$–R_F/SiO_2 nanocomposite encapsulated fullerene in water yielded a brown transparent solution related to the presence of fullerene, as shown in Figure 7B, while the corresponding PSt–VinylSi grafted R_F–$(ACA)_n$–R_F/SiO_2 nanocomposites yielded a colorless transparent solution (Figure 7A). UV–vis spectra of the well-dispersed aqueous solutions of PSt–VinylSi grafted R_F–$(ACA)_n$–R_F/SiO_2 nanocomposites-encapsulated fullerene are shown in Figure 8.

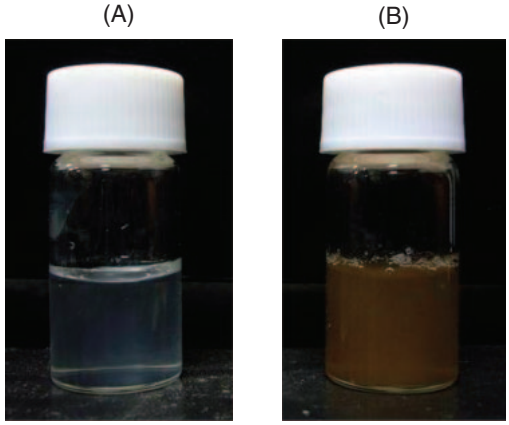

Figure 7. Photographs of aqueous solutions of PSt–Vinyl*Si* R_F–$(ACA)_n$–R_F/SiO_2 nanocomposites (Run 2 in Scheme 2) in the presence of C_{60} (B) and in the absence of C_{60} (A).

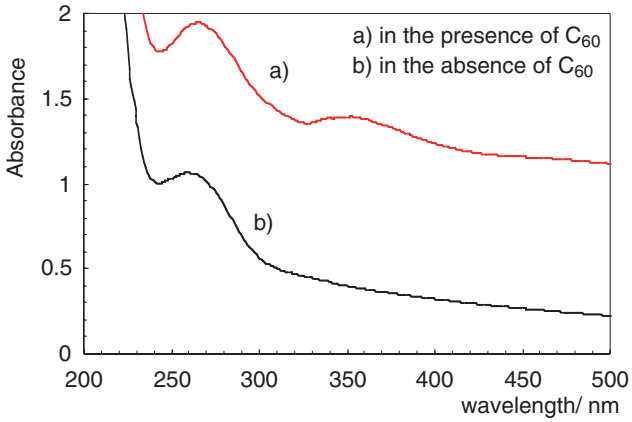

Figure 8. UV–vis spectra of aqueous solutions of PSt–Vinyl*Si* grated R_F–$(ACA)_n$–R_F/SiO_2 nanocomposites (Run 2 in Scheme 2) in the presence and the absence of C_{60}. Dispersion conditions: conc. of nanocomposite: 2.5 g dm^{-3}, 2 mL; C_{60}: 2 mg, stirring conditions: 2 h at room temparature.

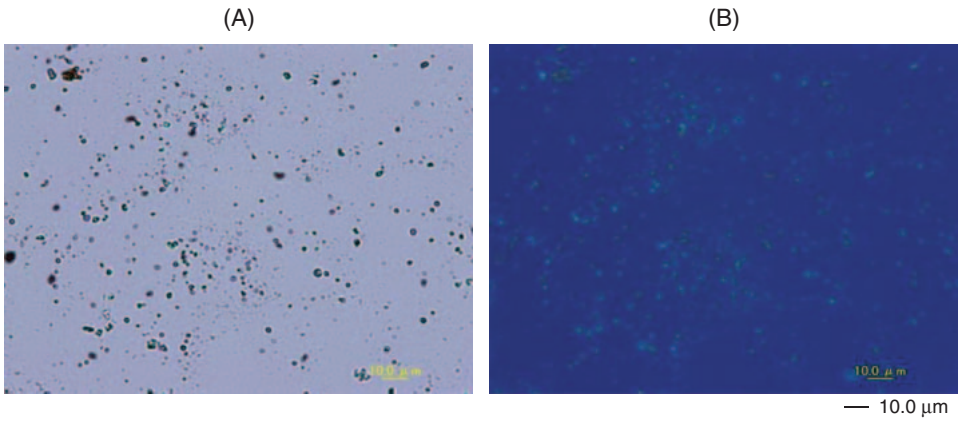

Figure 9. Optical microscopy (A) and fluorescence microscopy (B) images of aqueous solutions of fullerene in the presence of PSt–Vinyl*Si* R_F–$(ACA)_n$–R_F/SiO_2 nanocomposites (Run 2 in Scheme 2).

The PSt–Vinyl*Si* grafted R_F–$(ACA)_n$–R_F/SiO_2 nanocomposites-encapsulated fullerene showed a clear absorption band at around 350 nm related to fullerene. The amount of encapsulated fullerene in this nanocomposite was estimated by the use of the molar absorption coefficient (ε) 49000 (340 nm) of fullerene cited in the case of poly(vinylpyrrolidone),[17] and the encapsulated fullerene into nanocomposite was 15 μg mL^{-1}. DLS measurements show that the size of PSt–Vinyl*Si* grafted R_F–$(ACA)_n$–R_F/SiO_2 nanocomposites in water can increase effectively from 91.0 to 376 ± 73 nm through the encapsulation of fullerene into the grafted polymer network cores. Moreover, the optical micrograph showed that PSt–Vinyl*Si* grafted R_F–$(ACA)_n$–R_F/SiO_2 nanocomposites form fine submicrometer size-controlled particles (Figure 9A). Fluoresence imaging showed these particles to be light blue in color due to the presence of fullerene, which can exhibit fluorescence in the particle cores (Figure 9B) These findings suggest that fullerene should be tightly encapsulated into the grafted polymer network cores on the silica nanocomposite particle surfaces to afford new fluorinated silica nanocomposites containing fullerene in aqueous solutions.

We have studied the dispersion of fullerene into water by the use of other nanocomposites under similar conditions, and these results are shown in Figure 10.

As shown in Figure 10, PSt– and PDMAA–Vinyl*Si* grafted fluorinated nanocomposites were able to increase the amounts of encapsulated fullerene, effectively, compared to those of the corresponding MAcryl*Si* grafted and parent fluorinated nanocomposites containing Vinyl*Si* and MAcryl*Si* groups. This finding suggests that since vinylsilanes show in general poor radical copolymerization compared to that of methacrylates, grafted PSt–Vinyl*Si* or PDMAA–Vinyl*Si* segments can form more suitable host moieties to interact with fullerene as a guest molecule on the silica nanocomposite surfaces than that of PSt–MAcryl*Si* and PDMMA–MAcryl*Si*. Interestingly, PSt grafted fluorinated nanocomposites were found to exhibit higher encapsulation of fullerene than PDMAA grafted composites. This would be in part due to the effective van der Waals interaction between grafted PSt segments and fullerene.

We have studied the dispersion of SW-CNT into water by using PSt grafted fluorinated nanocomposites under similar

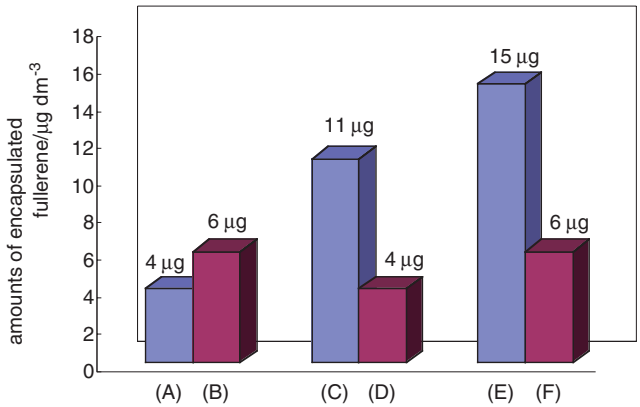

Figure 10. The amounts of encapsulated fullerene in PSt or PDMAA grafted R_F–$(ACA)_n$–R_F/SiO_2 nanocomposites. (A): R_F–$(ACA)_n$–R_F/SiO_2 nanocomposites containing Vinyl*Si* groups, (B): R_F–$(ACA)_n$–R_F/SiO_2 nanocomposites containing MAcryl*Si* groups, (C) PDMAA–Vinyl*Si* grafted R_F–$(ACA)_n$–R_F/SiO_2 nanocomposites (Run 4 in Scheme 2), (D) PDMAA–MAcryl*Si* grafted R_F–$(ACA)_n$–R_F/SiO_2 nanocomposites (Run 4 in Scheme 4), (E) PSt–Vinyl*Si* grafted R_F–$(ACA)_n$–R_F/SiO_2 nanocomposites (Run 2 in Scheme 2), (F) PSt–MAcryl*Si* grafted R_F–$(ACA)_n$–R_F/SiO_2 nanocomposites (Run 2 in Scheme 4). Conc. of nanocomposites: 2.5 g dm^{-3} (2 mL), fullerene (2 mg), stirring conditions: 2 h at room temparature.

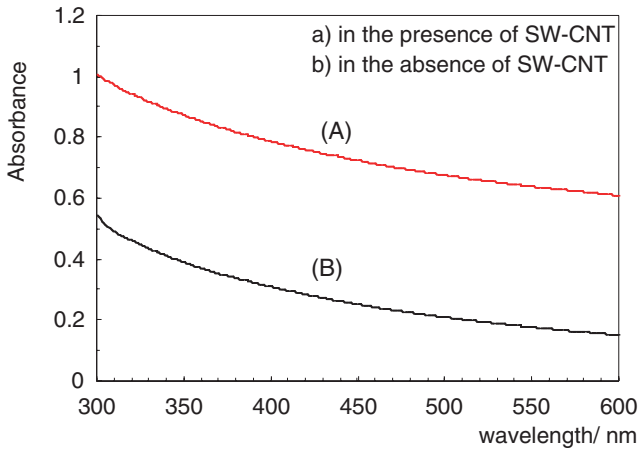

Figure 12. UV–vis spectra of aqueous solutions of PSt–Vinyl*Si* grafted R_F–$(ACA)_n$–R_F/SiO_2 nanocomposites (Run 2 in Scheme 2) in the presence (A) and the absence (B) of SW-CNT. Dispersion conditions: conc. of nanoparticle: 2.5 g dm^{-3} (2 mL), SW-CNT: 2 mg, stirring conditions: 2 h at room temparature.

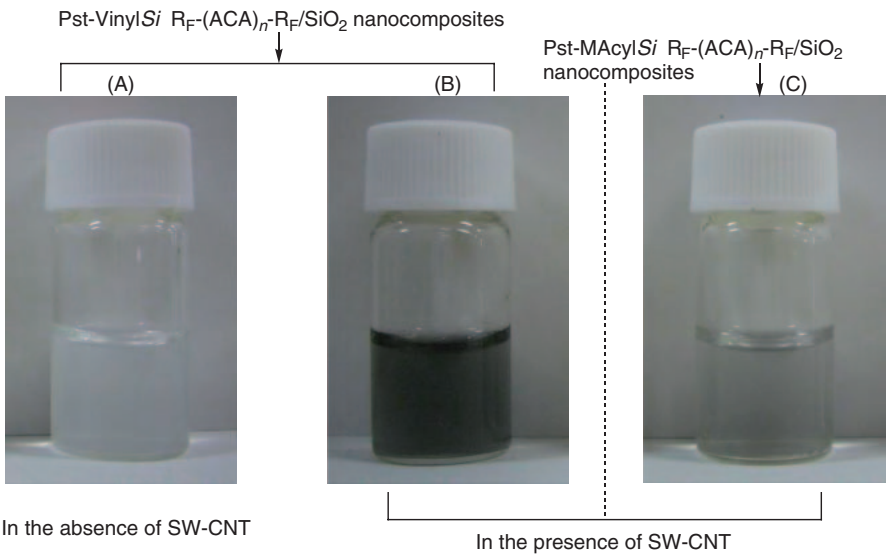

Figure 11. Photographs of aqueous solutions of PSt–Vinyl*Si* or MAcryl*Si* grafted R_F–$(ACA)_n$–R_F/SiO_2 nanocomposites (Run 2 in Scheme 2 or Run 2 in Scheme 4) in the absence (A) and in the presence of SW-CNT [(B) and (C)].

conditions as that of fullerene, and the results are shown in Figures 11 and 12.

As shown in Figure 11, well-dispersed PSt grafted fluorinated nanocomposites (Figures 11B and 11C), especially, PSt–Vinyl*Si* grafted fluorinated nanocomposites (Figure 11B) gave a gray transparent solution after the dispersion of SW-CNT into water, while the parent PSt–Vinyl*Si* fluorinated nanocomposite yielded a colorless transparent solution (Figure 11A).

The relative amounts of dispersed SW-CNT in water were estimated by the optical density at 500 nm (Figure 12) with the use of the molar absorption coefficient (ε) of SW-CNTs–*o*-dichlorobenzene solutions reported by Smalley et al.[18] The relative amounts of dispersed SW-CNT were shown in Table 4.

PSt–Vinyl*Si* grafted fluorinated nanocomposite was able to disperse SW-CNT in water effectively compared to that of PSt–MAcryl*Si*. This finding suggests that PSt–Vinyl*Si* grafted fluorinated nanocomposite should provide more suitable host moieties to interact with SW-CNT as a guest molecule in water. DLS measurements at 25 °C showed that the size of PSt–Vinyl*Si* grafted fluorinated nanocomposite in aqueous solutions was able to increase effectively from 91 to 404 nm by dispersion of SW-CNT, although the corresponding PSt–

Table 4. The Relative Amounts of Dispersed SW-CNT in Water

	Dispersed SW-CNT /μg mL^{-1}
PSt–Vinyl*Si* grafted composite	17
PSt–MAcryl*Si* grafted composite	4

MAcryl*Si* composite could not increase effectively its size (from 484 to 553 nm) by the dispersion of SW-CNT.

Conclusion

We have succeeded in preparing new PSt and PDMAA grafted fluoroalkyl end-capped acrylic acid oligomer/silica nanocomposites by the surface-initiated radical copolymerization of the corresponding fluorinated silica nanocomposite containing Vinyl*Si* and MAcryl*Si* groups with St or DMAA monomer. These PSt and PDMAA grafted fluorinated nanocomposites were found to exhibit good dispersibility in water and traditional organic solvents such as methanol, ethanol, tetrahydrofuran, and 1,2-dichloroethane. In these fluorinated naocomposite, PSt–Vinyl*Si* grafted fluorinated nanocomposite was found to be useful for new fluorinated polysoap, and this nanocomposite was able to disperse fullerene and carbon nanotubes more effectively into water, compared to other fluorinated silica nanocomposites.

Experimental

Measurements. Fourier-transform infrared (FTIR) spectra were measured using a Shimadzu FTIR-8400 FT-IR spectrophotometer (Kyoto, Japan), Ultraviolet–visible (UV–vis) spectra were measured by using a Shimadzu UV-1600 UV–vis spectrophotometer (Kyoto, Japan). Dynamic light-scattering (DLS) were measured by using an Otsuka Electronics DLS-7000 HL (Tokyo, Japan). Optical and fluorescence microscopies were measured by using an OLYMPUS Corporation BX51 (Tokyo, Japan). Scanning electron microscopy (SEM) images were measured by using a JEOL JSM-5300 (Tokyo, Japan). Thermal analyses were recorded on a Bruker axs TG-DTA2000SA differential thermobalance (Kanagawa, Japan). The ζ-potential was measured by the use of a Microtec Nition ZEECOM/ZC-2000 (Chiba, Japan).

Materials. Acrylic acid (ACA) and *N*,*N*-dimethylacrylamide (DMAA) were used as received from Toagosei Co., Ltd. (Tokyo, Japan) and Kojin Co., Ltd. (Tokyo, Japan), respectively. Styrene was purchased from Tokyo Kasei Kogyo Co., Ltd. (Tokyo, Japan). 2,2′-Azobis(2,4-dimethylvaleronitrile) (V-65) was purchased from Wako Pure Chemical Industries Ltd. (Osaka, Japan). SW-CNT (purity: 70–85%; diameter: 0.9–1.2 nm; length: 10–50 μm) was purchased from Sigma-Aldrich Japan Corp. (Tokyo, Japan). Fullerene (purity >99%) [C_{60}] was purchased from Tokyo Kasei Kogyo Co., Ltd. (Tokyo, Japan). Fluoroalkyl end-capped acrylic acid oligomer and *N*,*N*-dimethylacrylamide oligomer were prepared by reaction of fluoroalkanecarbonyl peroxide with the corresponding monomers according to our previously reported methods.[19,20]

Preparation of Fluoroalkyl End-Capped Acrylic Acid Oligomer/Silica Gel Nanocomposites Containing Vinyl*Si* Groups. To a methanol solution (25 mL) of fluoroalkyl end-capped acrylic acid oligomer {R_F–$(CH_2CHC(=O)OH)_n$–R_F [R_F–$(ACA)_n$–R_F]; $R_F = CF(CF_3)OCF_2CF(CF_3)OC_3F_7$; $M_n = 2630$ (0.50 g)}, were added tetraethoxysilane (TEOS: 0.20 mL), silica-nanoparticle methanol solution [30 wt %, 3.33 g; average particle size: 11 nm (Methanol Silica-sol (TR): Nissan Chemical Industrials Ltd., Tokyo, Japan)], 28% aqueous ammonia solution (0.5 mL), and trimethoxyvinylsilane (0.30 mL). The mixture was stirred with a magnetic stirring bar at room temperature for 2 h. After the solvent was evaporated off, to the obtained crude products was added methanol (25 mL). The methanol solution was stirred with magnetic stirring at room temperature for 2 days, and then was centrifuged for 30 min. The expected fluorinated nanocomposite was easily separated from the methanol solution. Fluorinated nanocomposite powders thus obtained were dried in vacuo at 50 °C for 2 days to afford purified particle powders (0.47 g). Fluoroalkyl end-capped acrylic acid oligomer/silica gel nanocomposites containing MAcryl*Si* groups were also prepared under similar conditions. The obtained nanocomposites were shown by the following FT-IR spectra characteristics.

R_F–$(ACA)_n$–R_F/SiO_2 nanocomposites containing Vinyl*Si* groups: FT-IR (ν/cm^{-1}) 3128 (OH), 2950 (CH), 1724 (CO), 1566 [CH_2=CHSi], 1240 (CF_2), 1111, 795 (SiO_2).

R_F–$(ACA)_n$–R_F/SiO_2 nanocomposites containing MAcryl*Si* groups: FT-IR (ν/cm^{-1}) 3132 (OH), 2966 (CH), 1717 (CO), 1588 [CH_2=CMe–], 1240 (CF_2), 1111, 814 (SiO_2).

Preparation of PSt–Vinyl*Si* Grafted Fluoroalkyl End-Capped Acrylic Acid Oligomer/Silica Gel Nanocomposites. Fluoroalkyl end-capped acrylic acid oligomer/silica gel nanocomposites containing Vinyl*Si* groups (0.20 g) in methanol (10 mL) were added to a mixture of styrene (2.0 g), 2,2′-azobis(2,4-dimethylvaleronitrile) (V-65: 0.3 g), a surfactant [R_F–$(CH_2CHCONMe_2)_n$–R_F; $R_F = CF(CF_3)OC_3F_7$: $M_n = 5010$; 0.4 g] and 1,2-dichloroethane (100 mL). The solution was stirred at 55 °C for 10 h under nitrogen. After centrifugal separation of this solution (2000 rpm/30 min), the obtained products were washed well several times with 1,2-dichloroethane, which well dissolves polystyrene. The isolated products were dispersed well in methanol with magnetic stirring at room temperature for 1 day, and then centrifuged for 30 min. The expected fluorinated nanocomposites were easily separated from the methanol solution. Fluorinated nanocomposite powders thus obtained were dried in vacuo at 50 °C for 2 days to afford purified particle powders (0.11 g). In the case of no surfactant use, we prepared PSt–Vinyl*Si* grafted fluoroalkyl end-capped acrylic acid oligomer/silica gel nanocomposites under similar conditions. Other PSt–MAcryl*Si* grafted, PDMAA–Vinyl*Si* grafted, and PDMAA–MAcryl*Si* grafted fluoroalkyl end-capped acrylic acid oligomer/silica gel nanocomposites were also prepared under similar conditions. The obtained nanocomposites were shown by the following FT-IR spectra characteristics.

PSt–Vinyl*Si* grafted R_F–$(ACA)_n$–R_F/SiO_2 nanocomposites (Run 2 in Scheme 2): FT-IR (ν/cm^{-1}) 3121 (OH), 2955 (CH), 1732 (CO), 1635–1600 (PSt), 1240 (CF_2), 1111, 799 (SiO_2).

PSt–MAcryl*Si* grafted R_F–$(ACA)_n$–R_F/SiO_2 nanocomposites (Run 2 in Scheme 4): FT-IR (ν/cm^{-1}) 3121 (OH), 2963 (CH), 1717 (CO), 1558 (PSt), 1243 (CF_2), 1111, 802 (SiO_2).

PDMAA–Vinyl*Si* grafted R_F–$(ACA)_n$–R_F/SiO_2 nanocomposites (Run 4 in Scheme 2): FT-IR (ν/cm^{-1}) 3121 (OH), 2955 (CH), 1717 (CO), 1636 (CO), 1245 (CF_2), 1111, 810 (SiO_2).

PDMAA–MAcryl*Si* grafted R_F–$(ACA)_n$–R_F/SiO_2 nanocomposites (Run 4 in Scheme 4): FT-IR (ν/cm^{-1}) 3300 (OH), 2951 (CH), 1732 (CO), 1620 (CO), 1240 (CF_2), 1111, 802 (SiO_2).

Dispersion of SW-CNT and Fullerene into Water by the Use of PSt–Vinyl*Si* Grafted R_F–$(ACA)_n$–R_F/SiO_2 Nanocomposites. To an aqueous solution of PSt–Vinyl*Si* grafted R_F–$(ACA)_n$–R_F/

SiO_2 nanocomposites ($2.5\,g\,dm^{-3}$: 2 mL) was added SW-CNT (2 mg). The mixture was stirred with a magnetic stirring bar at room temperature for 2 h. The aqueous solution thus obtained was centrifuged for 30 min to obtain a gray transparent solution. The relative amounts of dispersed SW-CNT in water were estimated by the optical density at 500 nm (UV–vis spectra) with the use of the molar absorption coefficient (ε) of SW-CNT–*o*-dichlorobenzene solution reported by Smalley et al.[18] and the relative amount of dispersed SW-CNTs was $17\,\mu g\,mL^{-1}$.

The amounts of dispersed fullerene into water were determined according to our previously reported method.[16]

References

1 a) *Functional Hybrid Materials*, ed. by P. Gomez-Romero, C. Sanchez, Wiley-VCH, Weinheim, **2004**. b) P. Judeinstein, C. Sanchez, *J. Mater. Chem.* **1996**, *6*, 511. c) J. Wen, G. L. Wilkes, *Chem. Mater.* **1996**, *8*, 1667. d) C. J. Brinker, G. W. Scherer, *Sol–Gel Science*, Academic Press, Boston, **1990**. e) M. Misra, A. Guest, M. Tilley, *Surf. Coat. Int., Part B* **1998**, *81*, 594. f) Z. Hua, K. Y. Qiu, *Polymer* **1997**, *38*, 521. g) M. A. S. Pedroso, M. L. Dias, C. Azuma, R. A. S. San Gil, C. G. Mothé, *Colloid Polym. Sci.* **2003**, *281*, 19. h) A. Bandyopadhyay, M. D. Sarkar, A. K. Bhowmick, *J. Polym. Sci., Part B: Polym. Phys.* **2005**, *43*, 2399. i) S. Li, Z. Zhou, H. Abernathy, M. Liu, W. Li, J. Ukai, K. Hase, M. Nakanishi, *J. Mater. Chem.* **2006**, *16*, 858.

2 a) P. Hajji, L. David, J. F. Gerard, J. P. Pascault, G. Vigier, *J. Polym. Sci., Part B: Polym. Phys.* **1999**, *37*, 3172. b) O. Prucker, J. Rühe, *Macromolecules* **1998**, *31*, 592. c) B. de Boer, H. K. Simon, M. P. L. Werts, E. W. van der Vegte, G. Hadziioannou, *Macromolecules* **2000**, *33*, 349.

3 a) B. Zhao, W. J. Brittain, *J. Am. Chem. Soc.* **1999**, *121*, 3557. b) R. Jordan, A. Ulman, J. F. Kang, M. H. Rafailovich, J. Sokolov, *J. Am. Chem. Soc.* **1999**, *121*, 1016.

4 S.-W. Zhang, S.-X. Zhou, Y.-M. Weng, L.-M. Wu, *Langmuir* **2005**, *21*, 2124.

5 a) R. Ranjan, W. J. Brittain, *Macromol. Rapid Commun.* **2008**, *29*, 1104. b) Y. Li, B. C. Benicewicz, *Macromolecules* **2008**, *41*, 7986. c) C.-H. Liu, C.-Y. Pan, *Polymer* **2007**, *48*, 3679. d) D. H. Nguyen, P. Vana, *Polym. Adv. Technol.* **2006**, *17*, 625.

6 a) C. Bartholome, E. Beyou, E. Bourgeat-Lami, P. Chaumont, N. Zydowicz, *Macromolecules* **2003**, *36*, 7946. b) M. Husseman, E. E. Malmström, M. McNamara, M. Mate, D. Mecerreyes, D. G. Benoit, J. L. Hedrick, P. Mansky, E. Huang, T. P. Russell, C. J. Hawker, *Macromolecules* **1999**, *32*, 1424.

7 a) K. Ueno, A. Inaba, M. Kondoh, M. Watanabe, *Langmuir* **2008**, *24*, 5253. b) K. Matyjaszewski, J. Xia, *Chem. Rev.* **2001**, *101*, 2921.

8 a) Y.-L. Liu, S.-H. Li, *Macromol. Rapid Commun.* **2004**, *25*, 1392. b) G. Schmid, *Nanoparticles*, Wiley-VCH, Weinheim, **2004**. c) L. Matejka, J. Plestil, *Macromol. Symp.* **1997**, *122*, 191. d) N. Juangvanich, K. A. Mauritz, *J. Appl. Polym. Sci.* **1998**, *67*, 1799.

9 a) B. Ameduri, B. Boutevin, *Well-Architectured Fluoropolymers: Synthesis, Properties and Applications*, Elsevier, Amsterdam, **2004**, pp. 231–348. b) K. Johns, G. Stead, *J. Fluorine Chem.* **2000**, *104*, 5. c) B. Ameduri, B. Boutevin, *J. Fluorine Chem.* **2000**, *104*, 53. d) J.-F. Berret, D. Calvet, A. Collet, M. Viguier, *Curr. Opin. Colloid Interface Sci.* **2003**, *8*, 296. e) P. Kujawa, C. C. E. Goh, D. Calvet, F. M. Winnik, *Macromolecules* **2001**, *34*, 6387. f) T. Imae, *Curr. Opin. Colloid Interface Sci.* **2003**, *8*, 307. g) L. Andruzzi, E. Chiellini, G. Galli, X. Li, S. H. Kang, C. K. Ober, *J. Mater. Chem.* **2002**, *12*, 1684. h) T. Imae, H. Tabuchi, K. Funayama, A. Sato, T. Nakamura, N. Amaya, *Colloids Surf., A* **2000**, *167*, 73. i) K. Jankova, S. Hvilsted, *J. Fluorine Chem.* **2005**, *126*, 241. j) P. Lebreton, B. Ameduri, B. Boutevin, J.-M. Corpart, *Macromol. Chem. Phys.* **2002**, *203*, 522. k) H. Sawada, *Chem. Rev.* **1996**, *96*, 1779. l) H. Sawada, T. Kawase, *Kobunshi Ronbunshu* **2001**, *58*, 147. m) H. Sawada, T. Kawase, *Kobunshi Ronbunshu* **2001**, *58*, 255. n) H. Sawada, *J. Fluorine Chem.* **2000**, *105*, 219.

10 L. Andruzzi, A. Hexemer, X. Li, C. K. Ober, E. J. Krame, G. Galli, E. Chiellini, D. A. Fischer, *Langmuir* **2004**, *20*, 10498.

11 H. Sawada, *Polym. J.* **2007**, *39*, 637.

12 H. Sawada, *Prog. Polym. Sci.* **2007**, *32*, 509.

13 H. Sawada, T. Narumi, A. Kajiwara, K. Ueno, K. Hamazaki, *Colloid Polym. Sci.* **2006**, *284*, 551.

14 a) H. Sawada, T. Narumi, S. Kodama, M. Kamijo, R. Ebara, M. Sugiya, Y. Iwasaki, *Colloid Polym. Sci.* **2007**, *285*, 977. b) H. Sawada, T. Tashima, S. Kodama, *Polym. Adv. Technol.* **2008**, *19*, 739. c) H. Sawada, H. Kakehi, T. Tashima, Y. Nishiyama, M. Miura, N. Isu, *J. Appl. Polym. Sci.* **2009**, *112*, 3482.

15 a) A. P. Philipse, A. Vrij, *J. Colloid Interface Sci.* **1989**, *128*, 121. b) Y. Wei, D. Yang, L. Tang, M. K. Hutchins, *J. Mater. Res.* **1993**, *8*, 1143.

16 a) H. Sawada, K. Shindo, J. Iidzuka, K. Ueno, K. Hamazaki, *Eur. Polym. J.* **2005**, *41*, 2232. b) H. Sawada, J. Iidzuka, T. Maekawa, R. Takahashi, T. Kawase, K. Oharu, H. Nakagawa, K. Ohira, *J. Colloid Interface Sci.* **2003**, *263*, 1. c) H. Yoshioka, M. Suzuki, M. Mugisawa, N. Naitoh, H. Sawada, *J. Colloid Interface Sci.* **2007**, *308*, 4.

17 Y. N. Yamakoshi, T. Yagami, K. Fukuhara, S. Sueyoshi, N. Miyata, *J. Chem. Soc., Chem. Commun.* **1994**, 517.

18 J. L. Bahr, E. T. Mickelson, M. J. Bronikowski, R. E. Smalley, J. M. Tour, *Chem. Commun.* **2001**, 193.

19 H. Sawada, Y.-F. Gong, Y. Minoshima, T. Matsumoto, M. Nakayama, M. Kosugi, T. Migita, *J. Chem. Soc., Chem. Commun.* **1992**, 537.

20 H. Sawada, Y. Yoshino, Y. Ikematsu, T. Kawase, *Eur. Polym. J.* **2000**, *36*, 231.